Tall Buildings and Damping: A Concept-Based Data-Driven Model

Seymour M. J. Spence[1] and Ahsan Kareem, A.M.ASCE[2]

Abstract: Modern tall buildings are characterized by their slenderness and sensitivity to resonant wind effects. This is especially true considering the acceleration-based motion perception criteria under which they must be designed. In light of the significance of the resonant response, damping plays an important role in the design of tall buildings. Unfortunately, unlike other mechanical characteristics of structures, damping is far more difficult to estimate. This is due to the inherent complexity and high number of mechanisms responsible for damping. For this reason, the experimental determination of damping levels for tall buildings from full-scale data collected during monitoring programs has obtained a tremendous amount of interest over the past years. This paper firstly reviews the predictive damping models that are available in the literature highlighting their merits and shortcomings in light of the extensive experimental damping data collected over the past few years. A novel amplitude-dependent data-driven model is then proposed based on a fully probabilistic description of the mechanisms that are hypothesized to generate the majority of damping in tall buildings. Finally, the proposed model is calibrated to a number of specific buildings demonstrating its robustness. **DOI: 10.1061/(ASCE)ST.1943-541X.0000890.**

Author keywords: Damping; Amplitude dependency; Data-driven models; Predictive models; Tall building design; Dynamic effects.

Introduction

The response of tall buildings to environmental loads, such as wind and seismic events, depends on their dynamic properties such as mass, stiffness, and damping. Although characteristics like mass and stiffness are fairly easy to estimate, damping is considerably harder to estimate with any sort of certainty. Being aware that this constitutes a difficulty in the design of structures, it is particularly significant in the case of tall buildings due to the stringent limitations imposed on their performance by acceleration-based motion perception criteria to guarantee a satisfactory habitability. The difficulty in obtaining accurate estimates of damping levels in civil structures may be traced back to the complex nature of the mechanisms that are at the root of this phenomenon. Indeed, it is well known that a structure will be dynamically damped by mechanisms with different characteristics. Examples of such mechanisms are the complex molecular interaction (material damping), Coulomb friction between members and connections or, from a more global perspective, other mechanisms depending on the type of structural system, foundation type, contributions of interior partitions, exterior cladding, and other nonstructural inputs. Damping is in general difficult to model mathematically because each of the aforementioned sources will follow very different laws (for instance, material damping may be modeled using viscous models, whereas a Coulomb model may be adopted for friction) causing the total damping to follow a law which may be considered unique for each structure. Having said this some general trends can be identified if parameters such as building material, structural system, and foundation type are considered.

In light of the importance and difficulties in modeling damping, the possibility, given by the development of data acquisition technologies over the last three decades, to experimentally determine damping characteristics from full-scale measurements has been thoroughly investigated. These studies have been made possible by a number of monitoring projects performed throughout the world on wind or seismically excited tall buildings (Jeary 1986; Ohkuma et al. 1991; Çelebi and Şafak 1992; Littler and Ellis 1992; Çelebi 1993; Tamura and Suganuma 1996; Li et al. 1998; Kijewski and Kareem 1999; Li et al. 2004b; Li et al. 2005; Li et al. 2006; Kijewski-Correa et al. 2006; Li et al. 2011; Guo et al. 2012), including the ongoing programs of the University of Notre Dame concerning the monitoring of three tall buildings in Chicago (Kijewski-Correa et al. 2006) and a number of tall buildings currently being monitored in China (Li et al. 1998; Li et al. 2003a; Li et al. 2004a; Li et al. 2008; Li et al. 2011; Guo et al. 2012). Obviously, the collection of full-scale data is only one part of the equation. Once the data have been collected, appropriate damping estimation techniques must be applied. Because of the considerable diversity that exists in today's buildings, together with the practical constraints placed on data acquisition systems (e.g., limited instrumentation points, noise, sensor accuracy), the number of methods that have been proposed for damping estimation is considerable (Kijewski-Correa and Cycon 2007).

Over the past three decades, one of the most interesting aspects of damping in tall buildings to have emerged from the analysis of full-scale data is its nonlinear nature. The nonlinearity is seen as a dependency of damping on the amplitude of vibration. This dependency, generally reported as an increase in damping with amplitude, has been the subject of numerous studies and investigations over the years (Hart and Vasudevian 1975; Daven port and Hill-Carroll 1986; Jeary 1986; Jeary 1996; Jeary 1997; Fang et al. 1999; Li et al. 2000b; Li et al. 2008; Li et al. 2011; Guo et al. 2012). Models have been proposed for predicting damping levels in function of vibration amplitude (Davenport and Hill-Carroll 1986;

[1]Research Assistant Professor, NatHaz Modeling Laboratory, Dept. of Civil and Environmental Engineering and Earth Sciences, Univ. of Notre Dame, Notre Dame, IN 46556 (corresponding author). E-mail: sspence@nd.edu

[2]Robert M. Moran Professor of Engineering, NatHaz Modeling Laboratory, Dept. of Civil and Environmental Engineering and Earth Sciences, Univ. of Notre Dame, Notre Dame, IN 46556.

Note. This manuscript was submitted on July 3, 2012; approved on June 4, 2013; published online on June 6, 2013. Discussion period open until July 6, 2014; separate discussions must be submitted for individual papers. This paper is part of the ***Journal of Structural Engineering***, © ASCE, ISSN 0733-9445/04014005(15)/$25.00.

Jeary 1986; Lagomarsino 1993; Jeary 1996; Jeary 1997; Satake et al. 2003). All the aforementioned models were proposed through the analysis of databases of damping values collected for various vibration amplitudes and buildings. Indeed, they may be considered as phenomenological models that have been given a certain physical sense a posteriori. Until recently this approach was the only realistic possibility. However, the increase of high quality damping estimates made on specific buildings for relatively large amplitude ranges has made possible the investigation of more concept-based damping models that would have a better chance of describing the damping behavior of tall buildings, explaining, for instance, why in certain cases damping has been seen to decrease after a certain critical amplitude (Tamura 2005; Smith and Willford 2007; Tamura and Yoshida 2008; Aquino and Tamura 2012). Another system nonlinearity that has been observed during the extensive monitoring of tall buildings over the past 12 years is the tendency for their natural frequencies to decrease to a certain extent with amplitude (Tamura and Suganuma 1996; Li et al. 2000a; Kijewski-Correa and Pirnia 2007; Kijewski-Correa et al. 2007). This has been seen to go hand in hand with the general increase of damping with amplitude. However, although this phenomenon has been observed and best-of-fit lines proposed for specific buildings, no models or theories have been proposed that bring these two phenomena together, as is mostly likely the case.

In light of the aforementioned considerations and the amount of data that has been collected over the past few years concerning tall buildings, the time seems right to investigate the possibility of defining specific concept-based data-driven models that are more robust and complete than those currently available. This paper focuses on this possibility.

Structural Damping

As briefly mentioned in the introduction, damping has many sources of varying complexity. It is the combination of various physical phenomena that causes damping to be particularly complicated to estimate, compared to mass or stiffness. Indeed, although the state variables that govern inertial forces or stiffness are easily identifiable, in the case of damping this is not true. Traditionally in the dynamic response analysis of structures damping is modeled proportional to velocity (linear viscous damping). In many cases, however, this choice is dictated more by convenience than by an actual physical meaning as with this choice the system will be governed by linear second-order differential equations.

Broadly speaking, damping affecting structures such as tall buildings may be categorized into structural damping and nonstructural damping. Structural damping comprises damping sources such as intrinsic material damping, frictional damping, and foundation damping due to soil-structure interaction. Nonstructural damping refers to all other sources such as aerodynamic damping, caused by the vibration of a structure immersed in a fluid (Kareem and Gurley 1996), or possible nonlinearities present in loading or structural system that may cause, for example, coupling between orthogonal modes with equal frequencies [this indirectly adds to the damping owing to an energy transfer between motion directions (Kareem 1982; Kareem and Gurley 1996)]. Although for certain systems nonstructural damping can be very important (for example aerodynamic damping on flexible structures), in general, for tall buildings it may be neglected for the current generation of buildings (Marukawa et al. 1996), but may have to be considered for supertall buildings of the future. Also, nonlinearities due to other aeroelastic effects or particular mechanical lock-in phenomena, such as those cited before, are presently rare, even if they may come into play in the supertall buildings that are being planned. This paper, therefore, will focus on the modeling and estimation of structural damping that will be referred to, from this point on, simply as damping.

For linear viscous damping, the ratio ξ between the damping present in the system and the critical damping may be estimated from the ratio between the dissipated energy in one cycle of resonant steady-state harmonic oscillation to the maximum amount of energy accumulated in the structure in that cycle

$$\xi = \frac{1}{4\pi}\left(\frac{\text{energy dissipated per cycle}}{\text{total available potential energy}}\right) \tag{1}$$

In the case of nonresonant harmonic loading, the linear viscous damping model has a serious drawback because the ratio of Eq. (1) depends on the exciting/steady-state response frequency, a characteristic not observed experimentally. Hence, for nonresonant harmonic loading, other damping models are probably more appropriate, such as the hysteretic damping model (complex stiffness damping) which is independent of the exciting/steady-state response frequency (Clough and Penzien 2003). Having said this, Eq. (1) is useful as a general definition of the damping capacity of a structure. Indeed, independently of the damping model, Eq. (1) provides a means to find what is commonly defined as the equivalent viscous damping ratio.

Damping: From Estimation to Databases

Full-Scale Monitoring Programs

The significant increase in knowledge concerning damping over the past 30 years is in part the consequence of the numerous monitoring programs that have been performed on buildings all over the world. This increased monitoring of the built environment has been made possible by the rapid advancement in acquisition technologies over the past few years and the growth of interest in structural health monitoring. The first cases of systematic monitoring of buildings under environmental loading occurred during the 1970s (Isyumov and Brignall 1975; Taoka et al. 1975; Isyumov et al. 1988; Brown 2003). Then during the 1980s programs such as the California Strong-Motion Instrumentation of Structures (CSMIS) of the California Geological Survey allowed the collection of a significant quantity of data related to the seismic response of buildings (Bongiovanni et al. 1987; Şafak 1989b; Çelebi and Şafak 1991; Şafak and Çelebi 1991; Çelebi and Şafak 1992; Çelebi 1993; Çelebi 1996). The last 20 years have seen a growing interest in the monitoring of wind-excited tall buildings (Li et al. 1998; Xu and Zhan 2001; Li et al. 2003a; Li et al. 2004a; Campbell et al. 2005; Li et al. 2005; Kijewski-Correa et al. 2006; Pirnia et al. 2007; Li et al. 2007; Kim et al. 2008; Li et al. 2008; Ni and Zhou 2010; Guo et al. 2012). This extensive monitoring and data analysis have been especially intense in the Pacific Rim where a number of buildings have been monitored, not only in ambient wind conditions, but also under severe weather conditions such as typhoons.

The Estimation of Damping

The collection of full-scale data is obviously only the first step in the experimental estimation of damping. Once the data has been collected an appropriate damping estimation technique must be applied. Because of the complexity of damping, this is by no means a trivial task. Indeed, in the literature a vast number of methods can be found. One of the most important factors in the selection of an appropriate method is whether the input (exciting function) was

measured during the event. Practically, this only happens in the case of seismic excitation, whereas for data collected during wind events only the response of the system is known. This makes a significant difference in the robustness of the techniques that may be applied.

Estimation under Seismic Excitation

In the case of known input, an appropriate System Identification (SI) technique may be applied for estimating the damping. The type of problem will in general be described by a nonlinear optimization problem, with scope the minimization of an objective function giving a measure of the difference between the model and measured responses. The methods are distinguished by the choice of the objective and the minimization scheme adopted (Kijewski-Correa and Cycon 2007). One of the more popular schemes is based on the regressive time-series modeling of the recorded input and output accelerations using the least squares minimization. The dynamic properties may then be extracted from the poles of the transfer function (Ljung 1987; Çelebi 1993). Another popular regression scheme is the AutoRegressive model with eXogenous input (ARX) which has been applied for the SI of a number of medium to tall buildings under seismic excitation (Şafak 1989b; Çelebi 1993; Çelebi 1996; Çelebi 2006; Rodgers and Çelebi 2006). In alternative, an ARMAX (AutoRegressive Moving Average model with eXogenous input) model may be used as illustrated in the identification of the Embarcadero building (Şafak 1989b). Another way to perform SI is to view the structure as a Discrete-Time Filter (DTF) that must be designed from the knowledge of the input and output (Şafak 1989a; Şafak 1991). This method has been successfully applied on a number of tall buildings (Şafak 1989b; Şafak 1991; Şafak and Çelebi 1991; Şafak and Çelebi 1992; Şafak 1993).

Estimation under Wind Excitation

As mentioned, the difference, from a system identification viewpoint, between wind and seismically excited structures is in the practical impossibility to measure the input forces in the case wind excitation. Also, owing to the relatively low amplitudes of the wind responses, damping estimation methods applied to wind response data must be capable of distinguishing between signal noise and response. Generally speaking, because the wind force may be considered broadband compared with the narrowband nature of the system, the input is taken as having a white noise spectrum around the structural frequencies. Also, it is common to assume the input as stationary and ergodic coupled with a linear system, therefore yielding a stationary and ergodic response. This allows the application of a number of output-only damping estimation schemes that allow for the damping estimation using temporal averages in place of ensambles (Kijewski-Correa and Cycon 2007).

Probably the most conventional technique that falls into this category is the Half Power BandWidth (HPBW) method (Bendat and Piersol 1987). The damping ratio is simply estimated from the auto power spectral density of the response at half the height. Some specific examples of its application can be found in (Dobryn et al. 1987; Brown 2003; Li et al. 2005; Kijewski-Correa et al. 2006; Kijewski-Correa et al. 2007; Pirnia et al. 2007). Other frequency domain-based schemes include spectral curve fitting methods and methods such as maximum likelihood estimators (Breukelman et al. 1993; Montpellier 1996; Erwin et al. 2007) or similar (Lagomarsino and Pagnini 1995).

Damping estimation in the frequency domain has been replaced to some extent by time domain procedures owing primarily to concerns about signal processing while applying the fast Fourier transforms which have been associated with inflated damping estimates. One of the first time domain-based damping estimation methods applied to full-scale wind excited buildings is based on the direct estimation of the autocorrelation function (Taoka et al. 1975; Isyumov and Halvorson 1984; Dobryn et al. 1987; Masciantonio et al. 1987). However, it has been seen that this method can give quite unreliable damping estimates if there is a lack of data (Davenport and Hill-Carroll 1986). The aforementioned difficulties are partly responsible for the popularity of the Random Decrement Technique (RDT) (Kareem and Gurley 1996). Not only has it been shown that this method is relatively stable in estimating damping, but also that it continues to be usable even when moderate nonlinearities and nonstationarities are present (Tamura and Suganuma 1996).

Discussion

The methodologies briefly presented in this section for damping estimation can significantly affect the values obtained. For this reason, when investigating possible trends in damping data coming from the application of different estimation techniques, the possibility of variation owing simply to the estimation method should not be overlooked. Indeed, recent studies have highlighted the advantages of working in the time-frequency domain through the Hilbert Transform (HT) or the Wavelet Transform (WT) (Kijewski et al. 2003; Xu et al. 2003; Bashor and Kareem 2007) because they have been seen to be far less sensitive to noise contamination compared with traditional approaches. They may also be adopted for damping estimation using short duration nonstationary data as shown in (Bashor and Kareem 2007; Kijewski-Correa and Cycon 2007) where single-value decomposition is applied together with WTs.

Databases

The continued monitoring and damping estimation has led to a number of damping databases being established over the years. Examples of such databases can be found in (Davenport and Hill-Carroll 1986; Lagomarsino and Pagnini 1995; Satake et al. 2003; Yoon and Ju 2004).

From the analysis of these databases, some important characteristics concerning the damping of steel and reinforced-concrete buildings have been found. A widely reported characteristic of damping established through the analysis of databases is the general increase of damping with frequency owing to the greater participation of nonstructural components to the damping of the system (Jeary 1986; Lagomarsino 1993; Satake et al. 2003). Over the years a number of researches have proposed predictive relationships concerning this phenomenon. In particular, Jeary (1986) proposed a relation between damping (ξ) and frequency in Hertz (n) expressed through the simple formula

$$\xi = 0.01n \tag{2}$$

whereas Tamura et al. (2000) proposed the following modification based on the results derived from analysis of the Japanese database [Architectural Institute of Japan (AIJ) 2000]

$$\begin{aligned} \xi &= 0.013n \quad \text{for steel frames} \\ \xi &= 0.014n \quad \text{for reinforced concrete} \end{aligned} \tag{3}$$

A more complicated relationship was proposed by Lagomarsino (1993)

$$\xi = \frac{\beta_1}{n} + \beta_2 n \tag{4}$$

where β_1 and β_2 are constants that depend on the principal building material (Lagomarsino 1993). By plotting modal frequency against the first three modal damping ratios in the lateral and

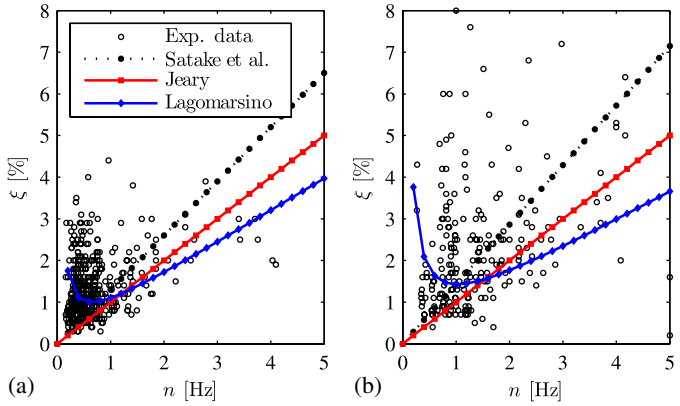

Fig. 1. Modal frequency against modal damping ratios in the first three modes: (a) steel framed buildings; (b) reinforced concrete buildings

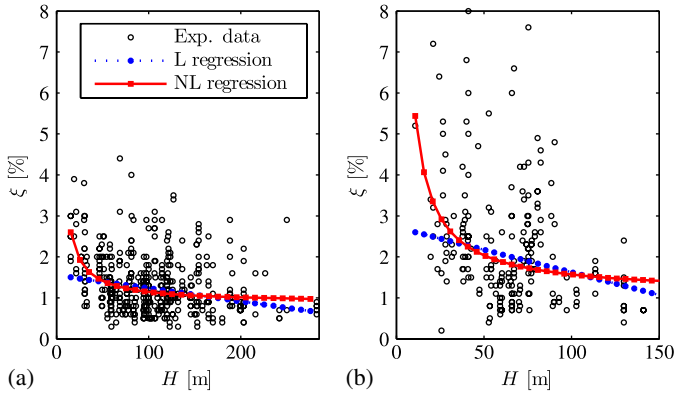

Fig. 2. Building height against modal damping ratios; the trend curves, fitted through linear (L) and nonlinear (NL) regression analysis, showing how damping is expected to reduce with building height: (a) steel-framed buildings; (b) reinforced-concrete buildings

torsional directions for the buildings in the Japanese database the frequency dependency is clearly visible for both steel-framed buildings, Fig. 1(a), and reinforced-concrete buildings, Fig. 1(b). In Fig. 1 the previously introduced damping-frequency relationships [Eqs. (2)–(4)] are also reported. Another characteristic that has emerged is the trend concerning the general reduction of damping in tall buildings with increasing height (Satake et al. 2003; Smith and Willford 2007), shown for the Japanese database in Fig. 2. This trend has led to some considering the possibility of using height as a desirable parameter for predictive damping models of tall buildings (Smith and Willford 2007), although this possibility is not shared by all (Bentz and Kijewski-Correa 2008).

Predictive Modeling and Amplitude Dependency of Damping

The investigation and definition of the mechanisms behind damping of typical multistory buildings owe a lot to the pioneering works of Hart and Vasudevian (1975), who were among the first to present the amplitude dependency of damping in reinforced concrete and steel multistory buildings, and Wyatt (1977) who presented a mechanism for its description through the introduction of elements termed *Stiction* (Stiction stands for a STuck frICTION element, in which, in the early stages of an increasing applied load, no motion takes place). From these early works more sophisticated models have been developed. The following sections will focus on arguably the most important of these proposals.

Power Law Model

Davenport and Hill-Carroll (1986) suggested that the mean or expected damping ratio in tall buildings may be estimated through a power law as

$$\xi = A\left(\frac{x}{H}\right)^{\alpha} \tag{5}$$

where A and α are constants, x is the standard deviation of the displacement (in mm) whereas H is the building height (in m).

The proposed mechanism behind the model is based on the assumption that the bulk of damping in built up structures is caused by the friction between joints, bearing plates, floors and beams, interior partitions, exterior cladding and structural system etc. The fact that this assumption leads to a law proportional to amplitude with constant exponent α, which is in contrast to the inverse dependency seen for Coulomb damping (Kareem and Gurley 1996), is demonstrated through the adoption of Wyatt's Stiction model (Wyatt 1977). In particular, it was suggested that the number of stick-slip elements increases in terms of the vibration amplitude with a power law of the type

$$u_x(x) = ux^{\alpha} \tag{6}$$

from which it can be demonstrated that the damping ratio will be given by

$$\xi = \frac{Dux^{\alpha}}{K(\alpha+1)(\alpha+2)} = \frac{DuH^{\alpha}}{K(\alpha+1)(\alpha+2)}\left(\frac{x}{H}\right)^{\alpha} = A\left(\frac{x}{H}\right)^{\alpha} \tag{7}$$

where K is the stiffness of the system while D and u are constants. The constants A and α may be estimated from experimental data derived from tests carried out on various building types, e.g., steel buildings or concrete buildings, therefore identifying the most appropriate values to be given to the constants (Davenport and Hill-Carroll 1986).

Piecewise Linear Model

Jeary (1986) proposed what has become, to a certain extent, the baseline for describing the mechanism behind damping in structures. The model is based on similar considerations as those cited for the power law model. As before, the model takes initial inspiration from the work of Wyatt (1977) by recognizing that the dominant cause of damping is friction-related and that this may be modeled through the use of the concept of stick-slip elements. However, the model is somewhat more complex in describing the origins behind the sources of energy dissipation.

In particular, the model is based on the definition of three distinct regions that define the amplitude dependency of damping. Namely, the regions are the constant low amplitude plateau, the nonlinear transition zone, and the constant high amplitude plateau. The existence of each zone is explained through the concept of critical shear stress associated with what are termed as imperfections. These last are considered at a material level as essentially microcracks and, at a structural level, as imperfections typified by dimensions in the order of meters (Jeary 1986; Jeary 1996; Jeary 1997). The macroimperfections are the result of the presence of construction joints, interface of structural elements, etc.

The existence of a low plateau region is then explained considering the shear energy necessary to activate dissipation mechanisms associated with the movement of structural imperfections. Because these are characterized by their relatively large dimensions, they are considered to have a low critical shear stress and therefore will be activated almost immediately. Before the material imperfections can be activated, a certain amplitude must be reached owing to the gap in the dimensions of the imperfections. This creates the constant low amplitude region. If the amplitudes are high enough, the elongation of the material imperfections will work as energy sinks causing an increase in the damping. The higher the amplitude the more of these imperfections will be activated causing the Stiction effect of the nonlinear damping region. At a certain amplitude all the material imperfections will be activated and the damping will become constant once again defining the high amplitude plateau. In general terms this model may be described by the following piecewise linear relationship:

$$\begin{array}{cc} \text{Low amplitude plateau} & \Rightarrow \xi = 0.01n \\ \text{Nonlinear region} & \Rightarrow \xi = 0.01n + 10^{\sqrt{D}/2}\left(\frac{x}{H}\right) \\ \text{High amplitude plateau} & \Rightarrow \xi = \xi_{\text{HA}} \end{array} \tag{8}$$

where x is the vibration amplitude (expressed in the same units as H), $0.01n$ is the low amplitude frequency-dependent damping value (with n expressed in Hz), D is the plan dimension of the building (expressed in m) whereas ξ_{HA} is the high amplitude damping value.

Modifications on the piecewise linear model have been proposed over the years. In particular Tamura et al. (2000) suggested slight modifications to Eq. (8) to take into account the modest differences seen in the amplitude-dependent damping characteristics of the buildings comprising the Japanese database, whereas Lagomarsino (1993) proposed the following modification:

$$\xi = \frac{\beta_1}{n} + \beta_2 n + \frac{\beta_3}{\lambda}\left(\frac{x}{H}\right) \tag{9}$$

where λ is the slenderness of the building taken as H/D and β_3 is a constant while x, H and D are expressed in consistent units.

Discussion

Both the power law and piecewise linear models were originally calibrated to databases. However, as high quality damping data over relatively significant amplitude ranges has become available, attempts have been made to fit Eq. (8) to specific building responses with varying degrees of success (Li et al. 2000b; Kijewski et al. 2003; Li et al. 2003b) while no specific attempt to fit Eq. (5) has been made. At this juncture it should be noted that both the aforementioned models are to a certain extent phenomenological. In particular, all the above-mentioned models consider damping as an amplitude increasing dynamic property of the system. However, there is evidence that, after reaching a critical amplitude, in some cases damping may actually start to decrease with amplitude (Tamura 2005; Smith and Willford 2007; Tamura and Yoshida 2008; Aquino and Tamura 2012). Also, together with amplitude-dependent damping, it has been widely reported that natural frequency will also become amplitude-dependent assuming steadily decreasing values (Tamura and Suganuma 1996; Li et al. 2000a; Kijewski-Correa and Pirnia 2007; Kijewski-Correa et al. 2007). At present, there are no models that are capable of describing in a general fashion these two phenomena. The aim of this paper is the proposal of a probabilistic concept-based data-driven model that is capable not only of providing a physical reason why damping may at times decrease with amplitude, but also of identifying the connection between amplitude-dependent frequency and damping.

Proposed Damping Model

The global behavior of tall buildings can be modeled by an equivalent dynamic system considering each floor to have three degrees of freedom (i.e., two orthogonal displacements and a rotation about a vertical axis). Under this assumption, the dynamic response of a tall building may be estimated by solving the following dynamic equilibrium equation:

$$\mathbf{M}\ddot{\mathbf{z}}(t) + \mathbf{C}\dot{\mathbf{z}}(t) + \mathbf{K}\mathbf{z}(t) = \mathbf{f}(t) \tag{10}$$

where $\mathbf{M}$, $\mathbf{C}$ and $\mathbf{K}$ are the mass, damping and stiffness matrices respectively, $\mathbf{z}$ is the Lagrangian response vector whereas $\mathbf{f}(t)$ is the vector of the time varying forcing functions acting at the reference center of each floor and evaluated as deemed appropriate by the analyst (e.g., if the wind response is of interest, then $\mathbf{f}(t)$ could be estimated by wind tunnel tests). In solving these equations, it is common to perform a modal analysis, truncated to the fundamental modes (first two translational modes and first torsional mode), and therefore replace the previous system with the following three uncoupled generalized equations of motion:

$$m_j\ddot{q}_j(t) + 2\zeta_j m_j\omega_j\dot{q}_j(t) + m_j\omega_j^2 q_j(t) = Q_j(t) \qquad j = 1,2,3 \tag{11}$$

where ζ_j is the generalized viscous damping ratio, $q_j(t)$ is the modal displacement, ω_j is the jth circular frequency whereas $Q_j(t)$ and m_j are the generalized force and mass, respectively.

In deriving Eq. (11), classical damping is generally assumed. However, as has been extensively presented, the assumption of classical damping is not always true for the response of most real buildings where damping is, among other things, amplitude-dependent. Also, as already mentioned, the natural frequencies of the building show a tendency to soften as the vibration amplitude increases. The possibility of capturing the aforementioned response characteristics while still describing the fundamental dynamic response through a reduced system of equations would seem of particular interest. To this end, the following paragraphs will present a damping model that implicitly assumes that the coupled equations of motion of Eq. (10) may be replaced by three independent nonlinear single degree of freedom dynamic equilibrium equations of the following form:

$$\begin{aligned} &M_i\ddot{x}_i(t) + C_i\dot{x}_i(t) + [K_i - \tilde{k}(\tilde{x}_i)]x_i(t) \\ &\quad + \hat{f}_i\int_0^\infty\int_0^{\tilde{x}_i} p_{f_0x_0}(\eta_1,\eta_2)d\eta_1 d\eta_2 = F_i(t) \quad i = 1,2,3 \end{aligned} \tag{12}$$

where M_i is the participating mass of the ith equation, C_i is the viscous material damping coefficient, $\ddot{x}_i(t)$, $\dot{x}_i(t)$ and $x_i(t)$ are the ith acceleration, velocity and displacement responses, K_i is the zero-amplitude stiffness, $\tilde{k}$ is the combined stiffness loss resulting from the slipping of the stick surfaces at the envelope amplitude of $\tilde{x}_i$, $\hat{f}_i$ is the total frictional damping force available to the ith equation whereas $p_{f_0x_0}(\cdot,\cdot)$ is the joint probability density function between the aleatory friction forces f_0, generated by the slipping surfaces, and the random vibration amplitudes, x_0, at which these surfaces become active. For all intents and purposes Eq. (12) plays an analogous role to Eq. (11) in describing the dynamic response of the building with, however, some added complexity that should allow the meaningful modeling of the experimentally observed amplitude-dependent damping and natural frequency. From a

physical standpoint, Eq. (12) is based on the widely accepted assumption that the source of amplitude-dependent damping may be traced back to the presence of a number of friction surfaces in the structure exhibiting stick-slip mechanisms. In particular, Eq. (12) defines a combined damping model because it also includes the contribution of the viscous material damping through the coefficient C_i. The contribution of this term is thought to be small compared to the frictional damping, but nevertheless important at lower amplitudes. What makes Eq. (12), and therefore the proposed damping model, different from other models that can be found in the literature is in how the frictional damping forces are modeled. In the proposed model, these are described by the joint probability density function between the random variables f_0 and x_0. Although the concept of randomly distributed slip forces has been considered previously (Davenport and Hill-Carroll 1986), the modeling of the amplitudes at which these forces will be initiated as a random variable has been until now overlooked. Traditionally, the amplitudes, x_0, are described by a deterministic function similar to that shown in Eq. (6). The ultimate consequence of the aforementioned assumption is that the number of slip surfaces will continue to grow indefinitely with amplitude, which goes against physical logic that would suggest the saturation of available slip surfaces as the vibration amplitudes increase (Bashor and Kareem 2008). Herein it is proposed to consider the amplitudes x_0 probabilistically distributed with appropriate law that will in general depend on the building under consideration. This probabilistic modeling of x_0 gives a physical meaning to the amplitudes and allows them to completely saturate as the vibration amplitude increases. The physical reasoning behind modeling x_0 as well as f_0 as random variables is understood by considering the sources of frictional forces in structural systems, i.e. at bolted joints, at bearing plates, in built-up elements, between floor and beams, at in-fill panels in frames, between frame and cladding, in microscopic material imperfections etc. All these sources are, to a greater or lesser extent, inevitable in buildings. Their unengineered nature obviously implies that they will be probabilistically distributed. In light of this, f_0 and x_0 can only be coherently modeled through the joint probability density function $p_{f_0x_0}(\cdot,\cdot)$ illustratively represented in Fig. 3. The ultimate result of this is that as $\tilde{x}_i$ increases the number of frictional sources activated

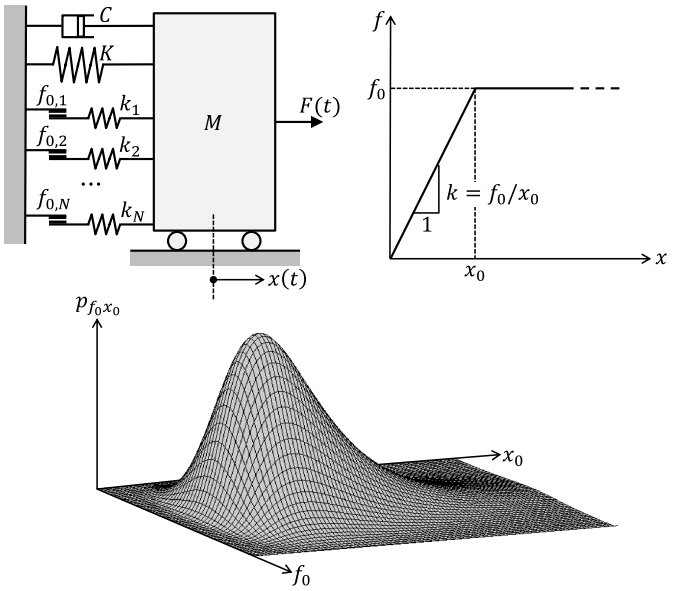

Fig. 3. Setting of Eq. (12)

will increase until, at saturation, they are all active. This is easily understood by recognizing that the double integral of the last term of the left-hand side of Eq. (12) is simply the cumulative distribution function of x_0 which will, by definition, tend to 1 as $\tilde{x}_i$ increases. The general setting of Eq. (12) is shown in Fig. 3.

Amplitude-Dependent Damping Ratio

In this section an expression for describing the amplitude-dependent damping ratio of Eq. (12) is searched. For the sake of clarity, for the remainder of this paper the subscript i will be dropped. To evaluate the damping ratio of Eq. (12), the expression reported in Eq. (1) may be invoked. In particular, for the combined system under investigation the total dissipated energy per cycle, ΔE_{tot}, may be written as

$$\Delta E_{\text{tot}} = \Delta E_{\text{vis}} + \Delta E_{\text{fric}} \tag{13}$$

where ΔE_{vis} is the energy dissipated due to viscous damping whereas ΔE_{fric} is the energy dissipated owing to friction. Although the calculation of ΔE_{vis}, and by consequence the viscous contribution to the damping ratio ξ_{vis}, does not present any particular difficulty, ΔE_{fric}, and so the frictional contribution to the damping ratio ξ_{fric}, is somewhat more difficult to estimate. This paragraph will focus on estimating ξ_{fric}.

Considering the single degree of freedom system of Eq. (12) under a steady-state vibration of amplitude $\tilde{x}$, the jth slipping surface of the system shown in Fig. 3 will dissipate per cycle a quantity of energy given by

$$\begin{aligned} &\Delta E_{\text{fric},j} = 4f_{0,j}(\tilde{x} - x_{0,j}) \quad \text{if } \tilde{x} > x_{0,j} \\ &\Delta E_{\text{fric},j} = 0 \quad \text{if } \tilde{x} \le x_{0,j} \end{aligned} \tag{14}$$

The total energy dissipated by the slipping surfaces at a vibration amplitude $\tilde{x}$ may then be written as

$$\Delta E_{\text{fric}} = 4N \int_0^{\infty} \int_0^{\tilde{x}} \eta_1(\tilde{x} - \eta_2) p_{f_{0x_0}}(\eta_1, \eta_2) d\eta_1 d\eta_2 \tag{15}$$

where N is the total number of stick-slip elements in the system. If the random variables f_0 and x_0 are considered independent, then their joint probability density function is given by $p_{f_0x_0}(\cdot,\cdot) = p_{f_0}(\cdot)p_{x_0}(\cdot)$ where $p_{f_0}(\cdot)$ is the probability density function of f_0 whereas $p_{x_0}(\cdot)$ is the probability density function of x_0. By introducing this simplification into Eq. (15) and by then taking advantage of the integration by parts rule, Eq. (15) may first be recast as

$$\Delta E_{\text{fric}} = 4N \int_0^{\tilde{x}} (\tilde{x} - \eta_2) p_{x_0}(\eta_2) d\eta_2 \int_0^{\infty} \eta_1 p_{f_0}(\eta_1) d\eta_1 \tag{16}$$

and then as

$$\Delta E_{\text{fric}} = 4N\bar{f}_0 \int_0^{\tilde{x}} \int_0^{\eta_2} p_{x_0}(\eta_1) d\eta_1 d\eta_2 \tag{17}$$

where $\bar{f}_0$ is the mean value of f_0. By invoking Eq. (1) the frictional component of the damping ratio ξ_{fric} of the nonlinear single degree of freedom oscillator of Eq. (12) may be written as

$$\xi_{\text{fric}}(\tilde{x}) = \frac{4N\bar{f}_0 \int_0^{\tilde{x}} \int_0^{\eta_2} p_{x_0}(\eta_1) d\eta_1 d\eta_2}{2\pi(K - \tilde{k}(\tilde{x}))\tilde{x}^2} \tag{18}$$

If the stiffness of the slip surfaces $\tilde{k}(\tilde{x})$ is considered small, as is expected, compared to the total stiffness of the structure K and by

collecting the independent terms together, the following expression can be derived for the amplitude dependent-damping ratio

$$\xi(\tilde{x}) = \xi_{\text{vis}} + A\frac{\int_0^{\tilde{x}}\int_0^{\eta_2} p_{x_0}(\eta_1)d\eta_1 d\eta_2}{\tilde{x}^2} \tag{19}$$

where A is a constant to be determined. To fix Eq. (19) the probability density function $p_{x_0}(\cdot)$ must be set as must the constant A and the viscous damping ratio ξ_{vis}.

Here it is proposed that x_0 be modeled as a lognormal random variable. This choice is particularly meaningful in light of the structure of Eq. (19). To better understand this last statement it is convenient to introduce the concept of critical amplitude, $\tilde{x}_{cr}$, defined as the amplitude at which Eq. (19) assumes its maximum value indicated with $\xi_{\max}$. With this in mind, Fig. 4(a), and more specifically Fig. 4(c), illustrate how the ratio between the critical amplitude $\tilde{x}_{cr}$ and the mode m_{x_0} of $p_{x_0}(\cdot)$ is constant as the mode m_{x_0} is varied once the standard deviation σ_{x_0} of the underlying normal distribution is fixed. This property is particularly significant as it allows the mode of the slip amplitude density to be fixed from the knowledge of $\tilde{x}_{cr}$ and σ_{x_0}. The relationship between σ_{x_0} and the aforementioned ratio, $\tilde{x}_{cr}/m_{x_0}$, is shown in Fig. 4(d). Fig. 4(b) illustrates the role of σ_{x_0} as a dimensionless shape parameter within the proposed damping model.

The aforementioned property allows the calibration of Eq. (19) to be achieved by first estimating the critical amplitude $\tilde{x}_{cr}$ and shape parameter σ_{x_0}. From the knowledge of σ_{x_0} and $\tilde{x}_{cr}$, the ratio $\tilde{x}_{cr}/m_{x_0}$ may be estimated from Fig. 4(d) therefore identifing m_{x_0}. The aforementioned procedure fixes $p_{x_0}(\cdot)$ leaving only ξ_{vis} and A to be found. After having fixed an appropriate value for ξ_{vis}, A may simply be identified by substituting into Eq. (19) the critical amplitude $\tilde{x}_{cr}$ and the corresponding damping ratio $\xi_{\max}$ and solving for A.

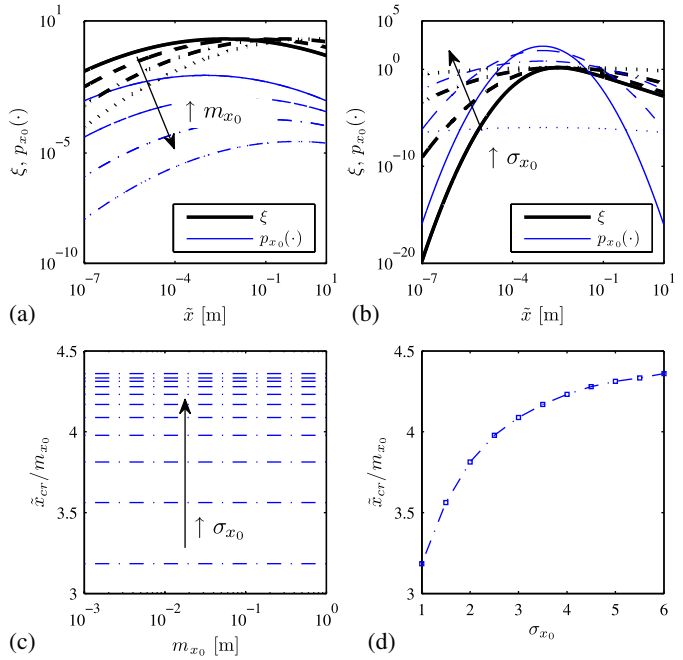

Fig. 4. Structure of Eq. (19) for $\xi_{\max} = 1.5\%$: (a) behavior of $p_{x_0}(\cdot)$ and $\xi(\tilde{x})$ for m_{x_0} varying between 10^{-3} m and 1 m, and with $\sigma_{x_0} = 4$; (b) behavior of $p_{x_0}(\cdot)$ and $\xi(\tilde{x})$ for $m_{x_0} = 10^{-3}$ m and σ_{x_0} varying between 1 and 6; (c) illustration of the constant nature of the ratio $\tilde{x}_{cr}/m_{x_0}$ for fixed values of σ_{x_0}; (d) illustration of the relationship between σ_{x_0} and $\tilde{x}_{cr}/m_{x_0}$, valid for any value of m_{x_0}

Amplitude-Dependent Frequency

The previous paragraph introduced a concept-based probabilistic model for describing the amplitude-dependent damping ratio of Eq. (12). In this section a relationship is searched for describing the amplitude-dependent stiffness of Eq. (12) with the aim of modeling how the vibration frequency is likely to vary with amplitude for the system schematically shown in Fig. 3.

As the amplitude of vibration increases, the number of slip surfaces that are slipping increases. This corresponds to a decreasing number of slip surfaces being able to provide stiffness. For an infinitesimal change in amplitude of vibration $d\tilde{x}$ and friction force df_0, the infinitesimal change in stiffness $d\tilde{k}$ may be written as

$$d\tilde{k} = N\frac{f_0}{\tilde{x}}p_{f_0}(f_0)p_{x_0}(\tilde{x})df_0 d\tilde{x} \tag{20}$$

where N is the total number of stick-slip surfaces. By integrating over all the force levels and up to a given amplitude, the following expression is found for the amplitude-dependent stiffness $\tilde{K}$ of the system of Eq. (12)

$$\tilde{K}(\tilde{x}) = K - N\int_0^{\infty}\int_0^{\tilde{x}}\frac{\eta_1}{\eta_2}p_{f_0}(\eta_1)p_{x_0}(\eta_2)d\eta_1 d\eta_2 \tag{21}$$

By first separating the variables in the double integral of the left-hand side of Eq. (21) and simplifying, the following expression for the amplitude-dependent stiffness is obtained:

$$\tilde{K}(\tilde{x}) = K - N\bar{f}_0\int_0^{\tilde{x}}\frac{p_{x_0}(\eta_2)}{\eta_2}d\eta_2 \tag{22}$$

Eq. (22) allows the following expression for the amplitude-dependent frequency n to be defined where it is assumed that the frequency at the amplitude $\tilde{x}$ depends on the stiffness at the same amplitude

$$n(\tilde{x}) = \frac{1}{2\pi}\sqrt{\frac{B_1 - B_2\int_0^{\tilde{x}}\frac{p_{x_0}(\eta_2)}{\eta_2}d\eta_2}{M}} \tag{23}$$

where $B_1 = K$ and $B_2 = N\bar{f}_0$ are constants to be estimated.

As in the case of the expression derived for the amplitude-dependent damping ratio, Eq. (23) depends on the probability density function $p_{x_0}(\cdot)$ of the slipping amplitudes. The dependency of both Eqs. (19) and (23) on $p_{x_0}(\cdot)$ is particularly interesting as it brings the amplitude-dependent damping and frequency properties together into a single model.

The calibration of Eq. (23) depends firstly on $p_{x_0}(\cdot)$, which may be derived from the calibration of Eq. (19), and on the choice of the constants B_1 and B_2. Although B_1 may, in theory, be estimated from accurate modeling of the zero amplitude stiffness, B_2 will in general need estimating from experimental data.

Application 1

In this section the proposed damping model will be calibrated to a selected number of tall buildings for which amplitude-dependent damping ratios and frequencies have been experimentally estimated through full-scale monitoring programs. All the experimental damping data were determined in the time domain using the RDT (Random Decrement Technique). To compare buildings with a range of heights, it is convenient to introduce the normalized amplitude indicated with $\underline{\tilde{x}} = (\tilde{x}/H)$ where H is the height of the building.

Table 1. Main Characteristics of the Calibrated Buildings

Building	H (m)	$D \times B$ (m)	Material	Use	System	Estimation method	Location
1	200	50×15	S	Mixed	SF	RDT	Japan
2	263	$\approx 60 \times 60$	RC	Residential	CO	RDT	South Korea
3	443	68×68	S	Office	SF	RDT	USA

Note: B = smallest plan dimension; CO = core and outrigger; D = largest plan dimension; RC = reinforced concrete; S = steel; SF = steel frame; SRC = steel/reinforced concrete.

Case Studies

Three buildings are considered whose main characteristics are reported in Table 1. The choice of these three buildings was made because of the availability of high quality and well documented amplitude-dependent and damping and frequency data (Kijewski-Correa et al. 2006; Kijewski-Correa and Pirnia 2007; Pirnia et al. 2007; Aquino and Tamura 2012) as well as their dramatically opposing behavior as vibration amplitude increases. Indeed, as is depicted in Fig. 5, buildings 2 and 3 show the classical increase of the damping ratio with amplitude whereas building 1, after an initial increase in damping with amplitude, shows a decreasing damping ratio with amplitude. This peculiar behavior cannot be explained through the adoption of classical damping models such as those reviewed in the section "Predictive Modeling and Amplitude Dependency of Damping" and has been the focus of recent studies (Aquino and Tamura 2012).

Calibration of the Proposed Damping Model to the Case Studies

Fig. 6 shows the results of the calibration of Eq. (19). As can easily be seen, the model shows very good agreement with the experimental data. Also, the capability of the proposed model in capturing the supposedly contradicting behavior between building 1 and buildings 2 and 3 is easily achieved. Within the setting of the proposed model, the difference seen in the amplitude-dependent characteristics may simply be ascribed to the significantly different distribution parameters of the slip amplitudes. Indeed, as shown in Fig. 7, buildings 2 and 3 have similar slip amplitude distributions, whereas building 1 has a significantly different distribution. Table 2 reports the model parameters obtained from the fitting of the three buildings. From this table it is interesting to observe the similarity between the model parameters, and, in particular, $m_{\underline{x}_0}$ and $\sigma_{\underline{x}_0}$, of buildings 2 and 3 as these are considered two buildings that exhibit a classical amplitude-dependent damping behavior. Therefore, in the realm of the proposed model it is expected that most buildings will have slip amplitude distributions similar to those of buildings 2 and 3.

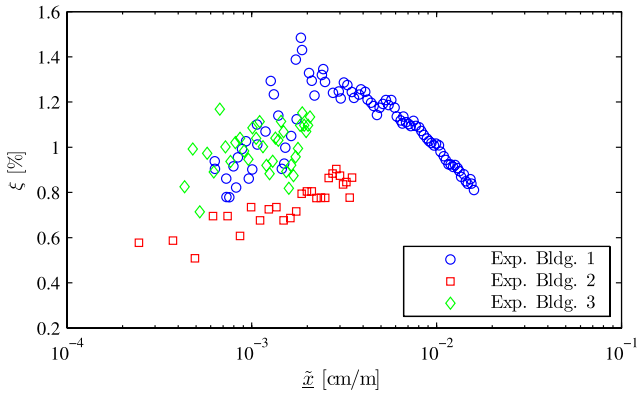

Fig. 5. Experimental amplitude-dependent damping characteristics for the first translational mode of the case study buildings

It is interesting to observe how the proposed damping model allows the prediction of the ξ_{max} representing the maximum expected damping ratio within the validity of Eq. (12). From Table 2 it can been seen that the proposed model is suggesting that building 3 will exhibit ξ_{max} around two times that of building 2.

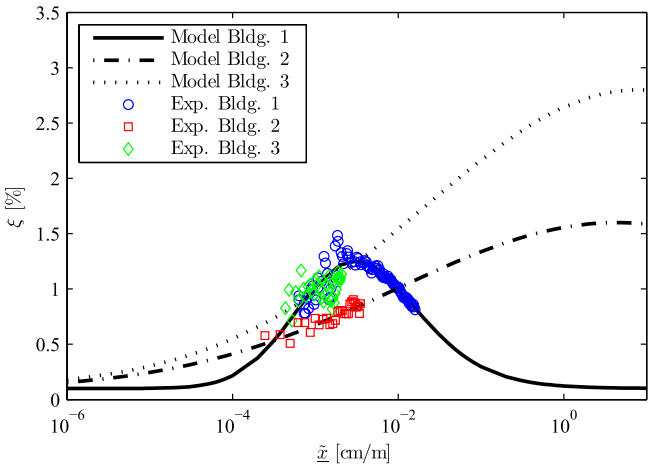

Fig. 6. Proposed amplitude-dependent damping model [Eq. (19)] fitted to the experimental damping data collected for the first translational mode of the case study buildings

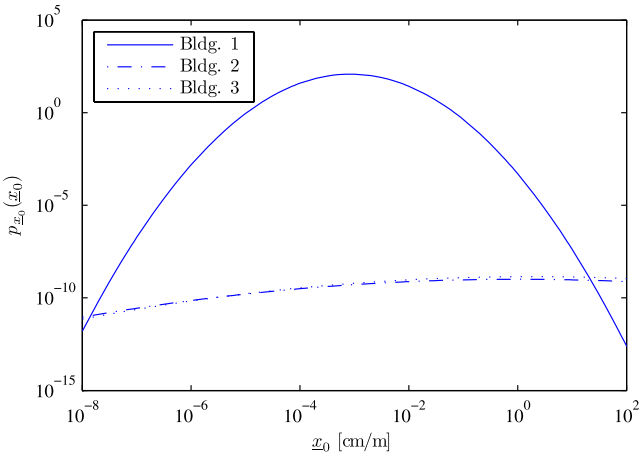

Fig. 7. Comparison between the fitted probability density functions $p_{\underline{x}_0}(\underline{x}_0)$ of the slip amplitudes for the case study buildings

Table 2. Model Parameters for Fitted Experimental Data

Building	$\tilde{x}_{cr}$ (cm/m)	ξ_{max} (%)	$m_{\underline{x}_0}$ (cm/m)	$\sigma_{\underline{x}_0}$	ξ_{vis} (%)	B_1 (kN/m)	B_2 (kN)
1	0.003	1.25	0.00085	1.42	0.1	1,228	0.89
2	4.3	1.6	1	6	0.09	619	2.72×10^{10}
3	7.74	2.8	1.8	5.85	0.11	3,000	2.80×10^{11}

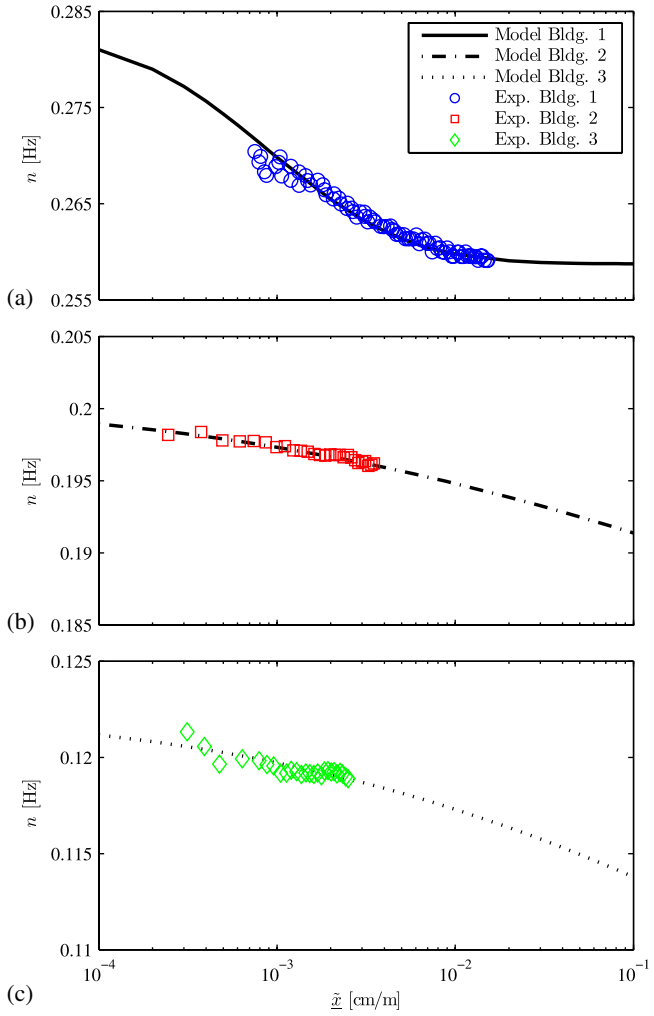

Fig. 8. Frequency-amplitude relationships predicted from the fitting of Eq. (23) to the experimental frequency-amplitude data of the case study buildings

This would seem in contrast to what could be expected considering the fact that building 2 has primarily residential use and reinforced concrete as structural material compared with building 3, which has primarily office use and steel as structural material (Table 1). A possible explanation for this could be the fact that building 3 would seem to have greater shear racking in its lateral deformation mechanism compared with building 2. Indeed, it has been suggested recently that the amount of shear racking compared with axial deformation (greater overall cantilever action) in the lateral deformation mechanism could play an important role in determining the overall damping capacity of tall buildings (Bentz and Kijewski-Correa 2008; Bentz 2012).

Fig. 8 shows the fitting of Eq. (23) to the amplitude-dependent frequency data collected for the case study buildings, whereas Table 2 shows the model parameter values. Once again the strong capability of the proposed model in reproducing the experimental data is very encouraging. Indeed, for all three buildings the amplitude-dependent frequency would seem to be easily reproduced by the proposed mechanism that attributes the loss of structural stiffness, as the amplitude increases, to the loss of stuck stick-slip surfaces. Close inspection of the frequency-amplitude behavior of building 1 (Fig. 8) gives particularly strong evidence of the validity of the proposed model. Indeed, if the hypothesis that the slip-stick surfaces are probabilistically distributed is true, then as the damping begins to saturate the frequency loss should begin to stabilize to a constant value as is effectively seen from the frequency-amplitude response of building 1.

Application 2

This section focuses on the calibration of the proposed model to the amplitude-dependent damping data of 12 tall buildings whose main characteristics are shown in Table 3. As can been seen the buildings, all of which are located in the Pacific Rim, apart from B2, B10, and B11, that are located in the United States (B11 in Chicago and B12 in Boston), have a good spread of heights and of principal construction material. The amplitude-dependent damping estimates for these buildings were obtained using the RDT, ensuring a certain consistency between the estimates.

Table 3. Main Characteristics and Fitted Model Parameters of the 12 Tall Buildings

Building	H (m)	Material	Mode	$\tilde{x}_{cr}$ (cm/m)	$\xi_{\max}$ (%)	$m_{\underline{x}_0}$ (cm/m)	$\sigma_{\underline{x}_0}$	ξ_{vis} (%)	R^2
B1	298	SRC	1	14.75	2.28	3.44	4.56	0.24	0.86
			2	14.61	1.75	3.35	6.13	0.00	0.90
B2	344	S	1	8.72	1.91	2.00	6.52	0.00	0.71
			2	11.70	1.42	2.67	8.42	0.00	0.67
B3	275	S	1	14.69	1.20	3.40	5.20	0.09	0.50
			2	20.14	1.13	4.70	4.60	0.21	0.32
B4	299	RC	1	15.76	1.34	3.59	9.01	0.00	0.88
			2	11.44	1.51	2.62	7.37	0.00	0.86
B5	297	RC	1	4.55	2.66	1.07	4.15	0.27	0.85
			2	1.47	3.50	0.35	3.75	0.17	0.91
B6	134	SRC	1	1.05	4.24	0.25	3.37	0.43	0.73
			2	2.22	4.20	0.53	3.84	0.43	0.86
B7	421	SRC	1	3.85	3.13	0.90	4.70	0.01	0.28
			2	1.70	3.23	0.40	4.40	0.01	0.43
B8	100	S	1	0.17	3.56	0.04	4.60	0.11	0.74
B9	197	RC	1	2.37	3.33	0.54	5.95	0.07	0.93
			2	2.22	3.46	0.51	6.03	0.05	0.93
B10	303	RC	1	3.95	4.22	0.91	5.34	0.21	0.76
			2	0.61	4.10	0.14	6.60	0.00	0.70
B11	443	S	1	3.11	3.20	0.72	5.12	0.05	0.32
			2	7.90	3.30	1.82	5.68	0.05	0.68
B12	246	S	1	0.88	3.00	0.21	3.60	0.07	0.79

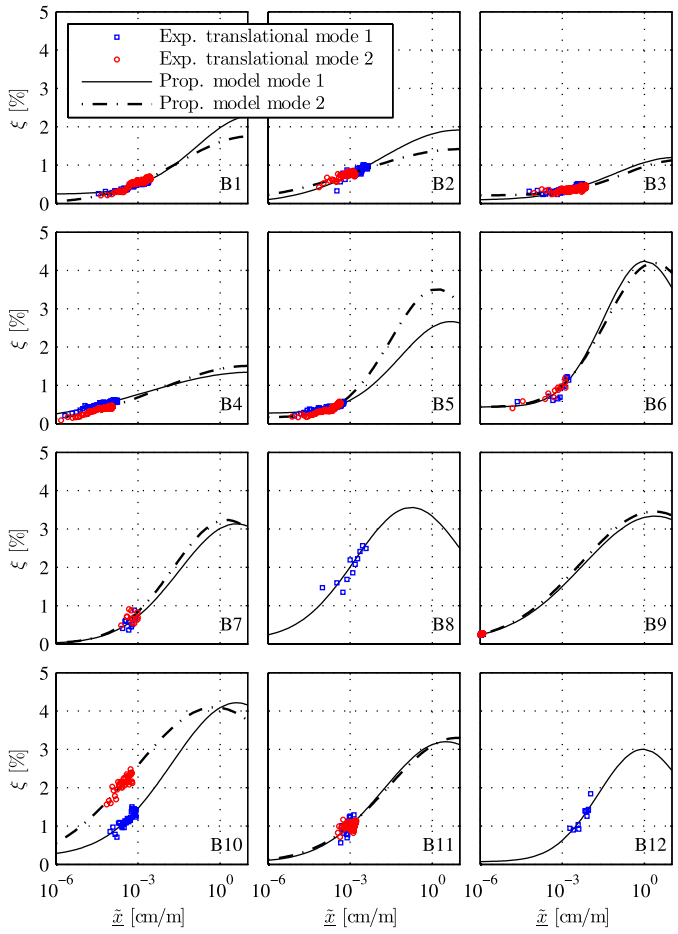

Fig. 9. Proposed model fitted to the amplitude-dependent experimental data of 12 representative tall buildings

Fig. 9 shows the proposed model fitted through a nonlinear least squares minimization to the first two orthogonal translational modes (when available) of the 12 buildings. The fitted model parameters for the 12 buildings are shown in Table 3. As can be seen, the model would seem easily capable of describing the amplitude-dependent damping characteristics of all the buildings. It is interesting to observe how the critical amplitude $\tilde{x}_{cr}$ (Table 3) is in general contained between 1 and 10, indicating the stability of the mode of the distribution of the slipping amplitudes $m_{\underline{x}_0}$. In other words, from the limited available data, the model is predicting that the maximum damping values will occur in roughly the same normalized amplitude range. This condition is obviously not satisfied by building 1 of Fig. 6. However, it is believed that the behavior of building 1 represents an anomaly in this respect. As more monitoring data comes available, this aspect will be further investigated.

The fitted experimental data of building B10 is worth commenting as the extremely different damping levels seen for the same amplitudes between the two modes has been the source of a number of discussions (Kijewski-Correa et al. 2007). As shown in Fig. 9, the model ascribes this difference simply to a difference in the slip amplitude distribution between the two orthogonal sway modes. Moreover, the model predicts that the maximum damping level between the two modes will be similar. It is also interesting to observe how buildings B1 to B4 have evidently lower $\xi_{\max}$ compared with buildings B5–B12 (Fig. 9 and Table 3). A possible explanation for this could be ascribed to the different lateral deformation mechanisms between the buildings. Indeed, it is expected that buildings B1–B4 have a predominantly cantilever action during lateral deformation, whereas buildings B5–B12 are expected to deform laterally following a predominantly frame racking action. As already mentioned, recent studies have suggested that this difference could possibly lead to significantly different maximum damping values (Bentz 2012).

In closing this section, it is worth noting that the model has been fitted to data collected over a limited range of amplitudes which obviously creates a certain amount of variability in the model predictions for amplitudes outside this range. For instance, the difference seen between the maximum damping ratios of the two lateral translational modes of building B5 may simply be due to a lack of data at higher vibration amplitudes. Nonetheless, the robustness of the proposed model reported in this section is extremely encouraging and suggests the validity of the model.

Proposed Damping Model as a Predictor Tool

This section focuses on the possibility of using the proposed damping model as a predictor and analysis tool for the estimation of amplitude-dependent damping ratios of tall buildings of height above 100 m. To investigate this possibility, an appropriate database of amplitude-dependent damping values is necessary.

Database of Amplitude-Dependent Damping Values

The database that was compiled for this study consists initially of 76 buildings of heights varying between 100 and 282 m extracted from the Japanese database (Satake et al. 2003), therefore ensuring a high quality of the damping values and associated amplitudes, because of the extensive data postprocessing that has been carried out (AIJ 2000; Satake et al. 2003). Together with these buildings, that consist mainly of steel-framed construction, an additional 19 buildings, with heights ranging from 100 to 443 m, with greater structural system and construction material variation are included in the database. The damping data for these last have been collected from the numerous publications that can be found in the literature reporting the results of the extensive monitoring programs presented in the section "Full-Scale Monitoring Programs" and concerning some landmark buildings in the United States as well as the Pacific Rim region. Finally, amplitude-dependent data of three tall buildings monitored during the CSMIS program of the California Geological Survey are also included in the database. The data points of these buildings consist of damping estimates made on notable steel-framed U.S. West Coast buildings, such as the Transamerica Tower (Çelebi and Şafak 1991; Şafak and Çelebi 1991), under high amplitude vibration during the Loma Prieta and San Fernando earthquakes (Beck and Jennings 1980; Şafak and Çelebi 1991; Çelebi 1993).

Each building in the database has one or two associated data points indicating amplitude-dependent damping estimates made for the first translational modes. A wide variety of system damping estimation methods were used under a number of naturally occurring and induced excitations. Table 4 reports the breakdown of excitation types used for estimating the damping ratios. Table 4 also reports the domain in which the damping was evaluated or whether a system identification method was used. As can be seen, the majority of the damping estimates were made in the time domain. In these cases, the prevalent method was the RDT. An important number of data points were obtained instead through frequency domain estimation techniques. In particular, a mixture of spectral curve fitting methods and the HPBW method were applied. Concerning the data points obtained from the application of SI

Table 4. Amplitude-Dependent Damping Database. Number of Data Points Classified by Excitation Type or Damping Evaluation Domain/System Identification

Excitation type/damping estimation technique	S	RC	SRC
IV	71	2	4
AV	39	12	13
EQ	16	1	4
TD	82	13	9
FD	26	2	8
SI	18	—	4

Note: IV = induced vibrations; AV = ambient vibrations; EQ = earthquake; FD = frequency domain; SI = system identification; TD = time domain.

techniques, the vast majority of the data was obtained through the implementation of ARMAX and ARX schemes with a few high amplitude data points coming from the application of a DTF scheme. The relatively broad spectrum of damping estimation techniques used for obtaining the points of the database will allow a preliminary investigation into possible differences seen in damping levels resulting simply from different estimation schemes.

Model Calibration and Discussion

Fig. 10 shows a Least Absolute Squares (LAR) fit of the proposed model to the database of the previous section, whereas Table 5 reports the model parameters derived from the LAR fit of the model to the database. Fig. 10 also compares the proposed model with the piecewise linear model, the modification proposed by Tamura et al. (2000), and the power law model. In plotting the piecewise linear model and its modification, the mean values of the data points concerning the natural frequencies and plan dimension D [Eq. (8)] in the direction of vibration are considered leading to smooth predictive curves. To illustrate the range of values that these models give considering the variation in natural frequency and plan dimension within the database, the maximum and minimum limits of the aforementioned models are also illustrated in Fig. 10. It should be observed also that for the model proposed by Tamura et al. (2000) moderately different coefficients were proposed for reinforced-concrete buildings compared with steel buildings. In the present comparison, only the predictive model concerning steel-frame structures is plotted because the large majority of the data points

Table 5. Parameters from LAR Calibration of the Proposed Model to the Databases

Parameter	Calibrated value
$\tilde{x}_{cr}$	5.72 cm/m
$\xi_{\max}$	3.23%
$m_{\underline{x}_0}$	1.33 cm/m
$\sigma_{\underline{x}_0}$	4.99
ξ_{vis}	0.45%

Note: Coefficient of determination, $R^2 = 0.48$.

in the database correspond to this structural type (Table 4). Also, in defining their model, Tamura et al. (2000) limited its range of applicability to a top drift ratio of no more than 2×10^{-3} cm/m and a maximum building height of 200 m. In the representation of the model presented in Fig. 10 the limit on drift ratio has been respected, although it should be observed that the database does contain a number of buildings with height greater than 200 m.

From the comparison of the aforementioned predictive damping models, it is evident how the proposed model is well capable of describing the amplitude-dependent characteristics of the database, whereas the piecewise linear model does not seem capable in this respect. It is also interesting to observe how for top drift ratios of less than 2×10^{-3} cm/m, the model proposed in (Tamura et al. 2000; Tamura 2012) has the closest correspondence to the proposed model, while for higher amplitudes the power law model seems to describe the database better than the piecewise linear. The similarity between the proposed model and the power law model in the high amplitude range can be ascribed to the underlying similarities between the philosophical standpoints of the two models. However, a fundamental and important difference between the two models lies in the way in which the proposed model behaves as higher amplitudes of vibration are encountered. Indeed, in the proposed model the saturation of the damping mechanisms causes the predictive curve to start to flatten out, whereas the power law model predicts ever increasing damping values. Fig. 10 also gives some validation of the proposed model in the high amplitude region. Indeed, in the calibration of the proposed model in section "Proposed Damping Model" there was very little data towards high amplitudes of vibration. The database of the present section, on the other hand, does contain some high amplitude data (Beck and Jennings 1980; Şafak and Çelebi 1991; Çelebi 1993). The similar values of the model parameters reported in Tables 2 and 3

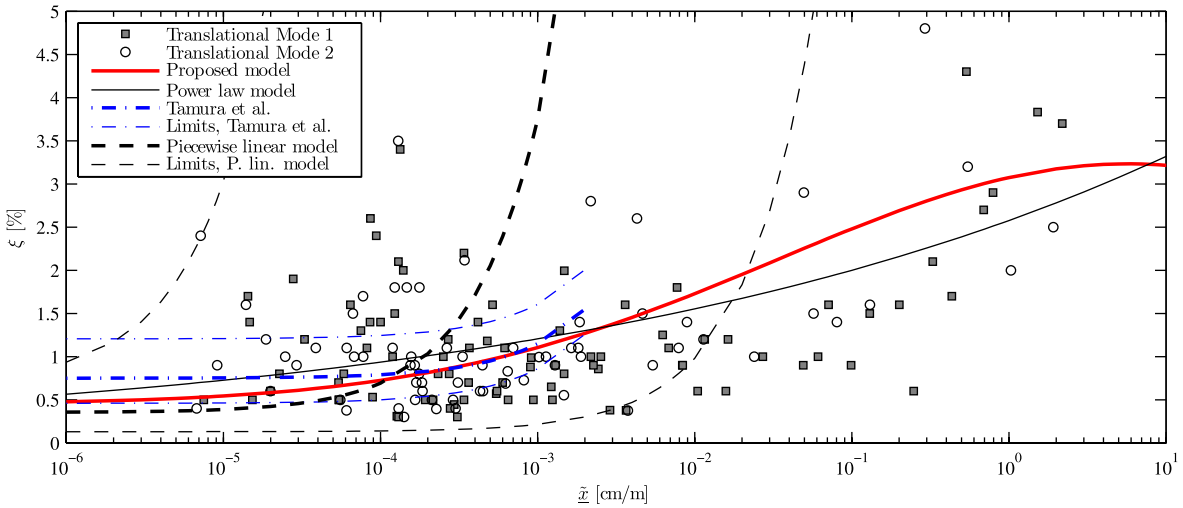

Fig. 10. Proposed model fitted to the database. Comparison with other amplitude-dependent damping predictor models

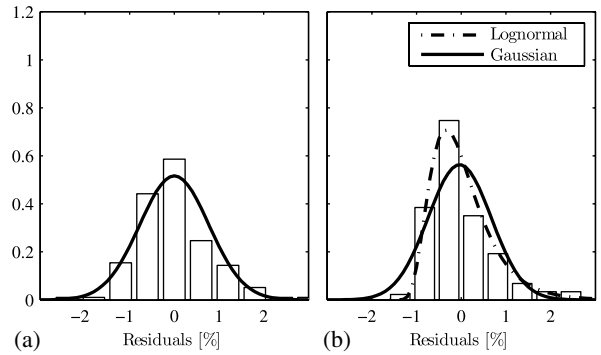

Fig. 11. Distribution of the residuals: (a) proposed model with fitted zero mean Gaussian distribution; (b) power law model with fitted lognormal distribution and comparison to a fitted Gaussian distribution illustrating the non Gaussian nature of the residuals

(with the exception of building 1 of Table 2) compared with those reported in Table 5 would seem encouraging as a first validation of the model in the high amplitude region.

Fig. 11(a) shows the estimated probability density function of the residuals of the data points. As can been seen, these are well estimated by a Gaussian distribution with zero mean, indicating the efficiency of the proposed model in describing the amplitude-dependent trend of the data. Indeed, the corresponding histogram concerning power law model, Fig. 11(b), clearly shows how the residuals of this model cannot be fitted by a zero mean Gaussian distribution.

Analysis of the Residuals

The residuals can be thought of as elements of variation unexplained by the fitted model, therefore their analysis can shed light on factors that may cause a particular building to be above or below the damping value predicted by a model. This section will explore this possibility with the aim of explaining some of the spread seen in the data.

Frequency, Material, and Height Dependency

As mentioned earlier in this paper, variation in damping levels between different buildings has often been linked to the differences in natural frequencies. This tendency can be seen in Fig. 12(a) where the difference in frequency between the various buildings (minimum 0.13 Hz and maximum 0.7 Hz) would seem to be weakly correlated with residuals taking on values above or below the trend curve. This would indicate that for the first two translational modes

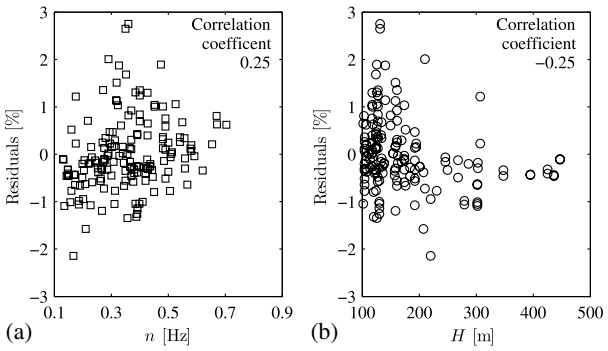

Fig. 12. Scatter plots showing: (a) residuals versus frequency; (b) residuals versus height

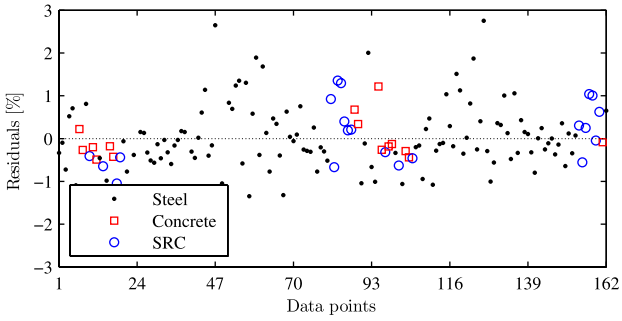

Fig. 13. Residuals in terms of predominant construction material

of tall buildings the dependency of damping on frequency does exists, although minimally. Obviously, the weak dependency on frequency of the first two translational modes may not hold for higher modes where greater frequency dependency may well exist. A similar result is seen concerning height [Fig. 12(b)] where a small but discernible relationship between height and damping would seem evident. The weak nature of these trends compared with what is normally observed (Tamura et al. 2000; Satake et al. 2003) is most likely resulting from the restriction placed on height ($H > 100$ m) for the buildings in the present database. Indeed, the results reported here do not conflict with those reported in (Tamura et al. 2000; Satake et al. 2003) where for buildings with height above 100 m the relationship between damping ratio and height is weaker than that seen for buildings of height less than 100 m. With this in mind, it would seem interesting to investigate other parameters that could complement height/natural frequency in determining appropriate damping values for buildings of height greater than 100 m.

Fig. 13 shows the residuals in terms of the predominant construction material. As can be seen, most buildings in the database are constructed from steel, however there would seem to be indication that concrete buildings tend to have greater damping values (seen as positive residuals) as compared with their steel counterparts. There would not seem to be any particular difference between steel and composite buildings.

Cantilever versus Shear Behavior

Recently it has been suggested that inherent damping levels of tall buildings can be related to the relative contribution of shear deformation (frame racking) versus axial deformation (cantilever action) (Kijewski-Correa et al. 2006; Erwin et al. 2007; Bentz and Kijewski-Correa 2008; Bentz 2012). In terms of the residuals, this concept translates into buildings that have a predominantly cantilever action taking on negative values and therefore being under the damping values predicted by the proposed model. This possibility is investigated in Fig. 14 where buildings with documented (Halvorson and Isyumov 1986; Bentz and Kijewski-Correa 2008; Bentz 2012) frame or cantilever action are highlighted as well as buildings for which the mode shapes are known allowing the classification to be carried out on the basis of the procedures proposed in (Bentz and Kijewski-Correa 2008; Bentz 2012). From this figure it would seem that buildings exhibiting a predominately cantilever lateral deformation mechanism do indeed have a reduced damping capability compared with buildings with a stronger shear racking frame action. It is also interesting to observe how the dividing line between the two behaviors is represented by more of a transition zone rather than a distinct jump confirming what was reported in (Bentz 2012).

Effects of the Damping Evaluation Technique. As highlighted in the section "The Estimation of Damping," there exists

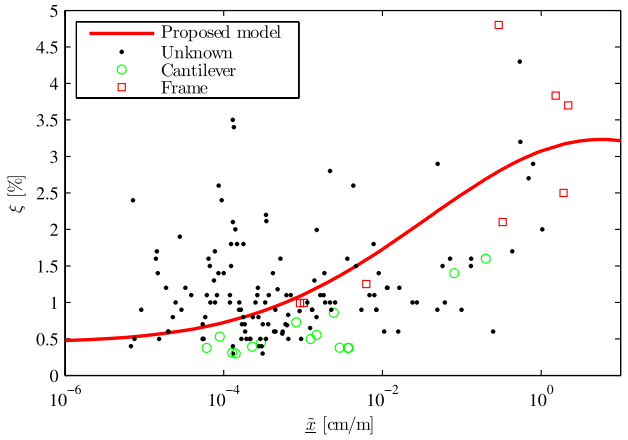

Fig. 14. Damping values of buildings with documented cantilever or frame action

a vast number of methods that have been proposed for estimating damping in structures. The highest level of separation between the various methods can be made in terms of whether damping is estimated in the frequency domain, time domain or if input and output are known allowing a system identification scheme to be used.

Table 6 reports the mean values of the residuals calculated on the damping estimates made under the aforementioned conditions. It is interesting to observe how the damping estimates made in the frequency domain would seem to be larger than their counterparts made in the time domain. This is also shown in Fig. 15 where it would seem evident that the frequency domain estimates tend towards more positive residuals indicating how damping estimates made in this domain would seem to be prone to overestimate, a concern also highlighted in Kijewski-Correa and Pirnia (2007).

Table 6 also reports a negative mean for the residuals of data estimated using SI methods. It is however difficult to draw any firm conclusions from this, as the residuals are seen to take on both positive and negative values (Fig. 15) indicating that this result could simply be due to a lack of data points.

Table 6. Effects of How Damping is Evaluated

Damping estimation technique	Mean values of the residuals
TD	−0.03
FD	0.36
SI	−0.42

Note: FD = frequency domain; SI = system identification; TD = time domain.

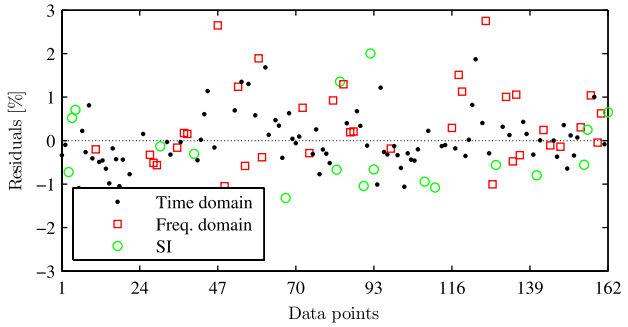

Fig. 15. Comparison between the residuals in terms of different damping evaluation methods

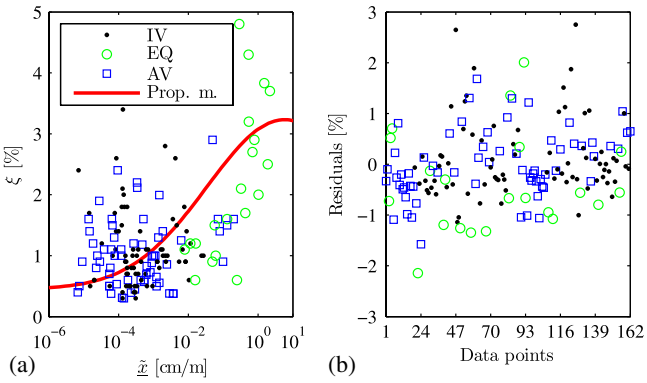

Fig. 16. Damping estimates in terms of excitation type: (a) amplitude-dependent estimates; (b) distribution of the residuals

Ambient Vibration, Induced Vibration, and Earthquake

Fig. 16(a) shows the distribution of the estimated damping values around the proposed damping model in terms of the excitation type, whereas Fig. 16(b) shows the distribution of the residuals. It is interesting to observe how damping estimates made under induced vibrations (IV) and ambient vibrations (AV) give a good spread of data points around the predicted values of the proposed model with mean values of the residuals equal to 0.11% and −0.01%, respectively. This is not the case for damping estimates made from earthquake records which have a mean value of the residual equal to −0.41%. This result is particularly interesting as it is generally expected that damping estimates made from seismic records will be more reliable than estimates made under other excitations as SI methods can be used for their estimation. This result is in line with what was reported in the previous section, and could be suggesting an overestimate of damping values made with output-only schemes at low vibration amplitudes. However, the small dimension of the dataset must be kept in mind when making such an assertion.

Conclusions

In this paper a novel concept-based data-driven probabilistic damping model was presented for describing the experimentally observed amplitude-dependent damping characteristics of tall buildings. In particular, the model may be considered combined as it takes into account both the viscous material damping as well as the predominant frictional damping of buildings. The model was extended so as to also describe, within a single theory, the dependency of natural frequency on vibration amplitude that has been widely reported in the literature together with amplitude-dependent damping. Expressions were derived for estimating the amplitude-dependent damping ratios and natural frequencies of the proposed model. Initial validation of the model was carried out on high fidelity experimental data collected on three tall buildings with dramatically opposing amplitude-dependent damping characteristics that are unexplainable by current models. The proposed model was seen to easily fit both the amplitude-dependent damping and frequency data. The capability of the model in describing the supposedly contradictory experimental data may be ascribed to its concept-based nature, and in particular the idea of eventual saturation of the damping sources as vibration amplitude increases. The model was further validated through its calibration to the experimental data derived on 12 tall buildings for their first two sway modes. Again the model was seen to be exceptionally robust and capable of shedding light on some seemingly contradictory experimental results. Finally, the model was calibrated as a predictive and analysis tool

to a specifically compiled database of amplitude-dependent damping data for tall buildings with heights varying between 100 and 450 m. The model was used as an amplitude corrector tool for the damping data therefore allowing a detailed study of the resulting residuals. From this investigation, it would seem that height is not a good predictive parameter for tall buildings. Instead it would seem as though the predominant lateral deformation mechanism, and therefore the structural system, plays an important role in deciding the damping capacity of tall buildings. Finally, the variation in experimentally determined damping values due to different estimation techniques was investigated, reaffirming the tendency for frequency domain estimates to be higher than time domain estimates.

Acknowledgments

Support was in part provided by the Tall Building Monitoring Program at the University of Notre Dame supported by the NSF Grant No. CMMI 06-01143 and the Global Center of Excellence at Tokyo Polytechnic University, funded by MEXT.

References

Aquino, R. E. R., and Tamura, Y. (2012). "Damping based on EPP spring models of stick-slip surfaces." (CD–ROM), *13th Int. Conf. on Wind Eng.*, International Association for Wind Engineering (IAWE), Atsugi, Kanagawa, Japan.

Architectural Institute of Japan (AIJ). (2000). *Damping in buildings*, Tokyo, Japan.

Bashor, R., and Kareem, A. (2007). "Efficacy of time-frequency domain system identification scheme using transformed singular value decomposition." *12th Int. Conf. on Wind Eng.*, International Association for Wind Engineering (IAWE), Atsugi, Kanagawa, Japan, 543–550.

Bashor, R., and Kareem, A. (2008). "Uncertainty in damping and damping estimates: An assessment of database and data from recent full-scale measurements." *2008 Structures Congress*, Structural Engineering Institute (SEI), Reston, VA.

Beck, J., and Jennings, P. (1980). "Structural identification using linear models and earthquake records." *Earthquake Eng. Struct. Dyn.*, 8(2), 145–160.

Bendat, J. S., and Piersol, A. G. (1987). *Random data: Analysis and measurement procedures*, Wiley, New York.

Bentz, A. (2012). "Dynamics of tall buildings: Full-Scale quantification and impacts on occupant comfort." Ph.D. thesis, Univ. of Notre Dame, Notre Dame, IN.

Bentz, A., and Kijewski-Correa, T. (2008). "Predictive models for damping in buildings: The role of structural system characteristics." *2008 Structures Congress, 18th Analysis and Computation Specialty Conf.*, Structural Engineering Institute (SEI), Reston, VA.

Bongiovanni, G., Çelebi, M., and Şafak, E. (1987). "Seismic rocking response of a triangular building founded on sand." *Earthquake Spectra*, 3(4), 793–810.

Breukelman, B., Dalgleish, A., and lsyumov, N. (1993). "Estimates of damping and stiffness for tall buildings." *7th U.S. National Conf. on Wind Eng.*, Univ. of California, Los Angeles.

Brown, B. (2003). "Analysis of wind induced acceleration and pressure data from an eight hundred foot tower." M.S. thesis, Univ. of Notre Dame, Notre Dame, IN.

Campbell, S., Kwok, K. C. S., and Hitchcock, P. A. (2005). "Dynamic characteristics and wind-induced response of two high-rise residential buildings during typhoons." *J. Wind Eng. Ind. Aerodyn*, 93(6), 461–482.

Çelebi, M. (1993). "Seismic response of eccentrically braced tall building." *J. Struct. Eng.*, 10.1061/(ASCE)0733-9445(1993)119:4(1188), 1188–1205.

Çelebi, M. (1996). "Comparison of damping in buildings under low-amplitude and strong motions." *J. Wind Eng. Ind. Aerodyn.*, 59(2–3), 309–323.

Çelebi, M. (2006). "Recorded earthquake responses from the integrated seismic monitoring network of the Atwood building, Anchorage, Alaska." *Earthquake Spectra*, 22(4), 847–864.

Çelebi, M., and Şafak, E. (1991). "Seismic response of Transamerica building. I: Data and preliminary analysis." *J. Struct. Eng.*, 10.1061/(ASCE)0733-9445(1991)117:8(2389), 2389–2404.

Çelebi, M., and Şafak, E. (1992). "Seismic response of Pacific Park Plaza. I: Data and preliminary analysis." *J. Struct. Eng.*, 10.1061/(ASCE)0733-9445(1992)118:6(1547), 1547–1565.

Clough, R., and Penzien, J. (2003). *Dynamics of structures*, Computers & Structures, Berkeley, CA.

Davenport, A. G., and Hill-Carroll, P. (1986). "Damping in tall buildings: Its variability and treatment in design." *Building motion in wind*, N. Isyumov and T. Tschanz, eds., ASCE, New York, 42–57.

Dobryn, C., Isyumov, N., and Masciantonio, A. (1987). "Prediction and measurement of wind response: Case story of a wind sensitive building." *Structures Congress 87 related to Dynamics of Structures*, J. M. Roesset, ed., Univ. of Texas, Civil Eng. Dept., Austin, TX.

Erwin, S., Kijewski-Correa, T., and Yoon, S. W. (2007). "Full-scale verification of dynamic properties from short duration records." (CD–ROM), *2007 Structures Congress: New Horizons and Better Practices*, Structural Engineering Institute (SEI), Reston, VA.

Fang, J. Q., Li, Q. S., Jeary, A. P., and Liu, D. K. (1999). "Damping of tall buildings: Its evaluation and probabilistic characteristics." *Struct. Des. Tall Special Build.*, 8(2), 145–153.

Guo, Y. L., Kareem, A., Ni, Y. Q., and Liao, W. Y. (2012). "Performance evaluation of Canton Tower under winds based on full-scale data." *J. Wind Eng. Ind. Aerodyn.*, 104–106, 116–128.

Halvorson, R., and Isyumov, N. (1986). "Comparison of predicted and measured dynamic behavior of Allied Bank Plaza." *Building motion in wind*, N. Isyumov and T. Tschanz, eds., ASCE, New York, 23–41.

Hart, G. C., and Vasudevian, R. (1975). "Earthquake design of buildings: Damping." *J. Struct. Div.*, 101(1), 11–30.

Isyumov, N., and Brignall, J. (1975). "Some full-scale measurements of wind-induced response of the CN Tower, Toronto." *J. Wind Eng. Ind. Aerodyn.*, 1, 213–219.

Isyumov, N., and Halvorson, R. A. (1984). "Dynamic response of Allied Bank Plaza during Alicia." *Hurricane Alicia: One year later*, A. Kareem, ed., ASCE, Seoul, 98–116.

Isyumov, N., Masciantonio, A., and Davenport, A. G. (1988). "Measured motions of tall buildings in wind and their evaluation." *Proc. of the Symp./Workshop on Serviceability of Buildings*, National Research Council Canada, Ottawa, ON, 181–199.

Jeary, A. P. (1986). "Damping in tall buildings, a mechanism and a predictor." *Earthquake Eng. Struct. Dyn.*, 14(5), 733–750.

Jeary, A. P. (1996). "The description and measurement of nonlinear damping in structures." *J. Wind Eng. Ind. Aerodyn.*, 59(2–3), 103–114.

Jeary, A. P. (1997). "Damping in structures." *J. Wind Eng. Ind. Aerodyn.*, 72, 345–355.

Kareem, A. (1982). "Acrosswind response of buildings." *J. Struct. Div.*, 108(4), 869–887.

Kareem, A., and Gurley, K. (1996). "Damping in structures: Its evaluation and treatment of uncertainty." *J. Wind Eng. Ind. Aerodyn.*, 59(2–3), 131–157.

Kijewski, T., Brown, D., and Kareem, A. (2003). "Identification of dynamic properties of a tall building from full-scale response measurements." (CD–ROM), *11th Int. Conf. on Wind Eng.*, International Association for Wind Engineering (IAWE), Atsugi, Kanagawa, Japan.

Kijewski, T., and Kareem, A. (1999). "Analysis of full-scale data from a tall building in Boston: Damping estimates." *10th Int. Conf. on Wind Eng.*, International Association for Wind Engineering (IAWE), Atsugi, Kanagawa, Japan.

Kijewski-Correa, T., et al. (2006). "Validating wind-induced response of tall buildings: Synopsis of the Chicago full scale monitoring program." *J. Struct. Eng.*, 10.1061/(ASCE)0733-9445(2006)132:10(1509), 1509–1523.

Kijewski-Correa, T., et al. (2007). "Full-scale performance evaluation of tall buildings under winds." *12th Int. Conf. on Wind Eng.*, International Association for Wind Engineering (IAWE), Atsugi, Kanagawa, Japan, 351–358.

Kijewski-Correa, T., and Cycon, J. (2007). "System identification of constructed buildings: Current state-of-the-art and future directions." (CD–ROM), *3rd Int. Conf. on Struct. Health Monitoring of Intelligent Infrastructure*, Structural Engineering Institute (SEI), Reston, VA.

Kijewski-Correa, T., and Pirnia, J. D. (2007). "Dynamic behavior of tall buildings under wind: Insights from full-scale monitoring." *Struct. Des. Tall Special Build.*, 16(4), 471–486.

Kim, J. Y., Kim, D. Y., and Kim, S. D. (2008). "Evaluations of the dynamic properties for a residential tall building in Korea." *CTBUH 8th World Congress*, Council on Tall Buildings and Urban Habitat (CTBUH), Chicago.

Lagomarsino, S. (1993). "Forecast models for damping and vibration periods of buildings." *J. Wind Eng. Ind. Aerodyn.*, 48(2–3), 221–239.

Lagomarsino, S., and Pagnini, L. C. (1995). "Criteria for modeling and predicting dynamic parameters of buildings." *Rep. No. ISC-II*, Istituto di Scienza Delle Costruzioni, Università di Genova, Facoltà di Ingegneria.

Li, Q., Xiao, Y. Q., Fu, J. Y., and Li, Z. N. (2007). "Full-scale measurements of wind effects on the Jin Mao Building." *J. Wind Eng. Ind. Aerodyn.*, 95(6), 445–466.

Li, Q. S., et al. (2006). "Wind tunnel and full-scale study of wind effects on China's tallest building." *Eng. Struct.*, 28(12), 1745–1758.

Li, Q. S., Fang, J. Q., Jeary, A. P., and Wong, C. K. (1998). "Full-scale measurement of wind effects on tall buildings." *J. Wind Eng. Ind. Aerodyn.*, 74–76(1), 741–750.

Li, Q. S., Fang, J. Q., Jeary, A. P., Wong, C. K., and Liu, D. K. (2000a). "Evaluation of wind effects on a supertall building based on full-scale measurements." *Earthquake Eng. Struct. Dyn.*, 29(12), 1845–1862.

Li, Q. S., Liu, D. K., Fang, J. Q., Jeary, A. P., and Wong, C. (2000b). "Damping in buildings: Its neural network model and AR model." *Eng. Struct.*, 22(9), 1216–1223.

Li, Q. S., Wu, J. R., Liang, S. G., Xiao, Y. Q., and Wong, C. K. (2004a). "Full-scale measurements and numerical evaluation of wind induced vibration of a 63-story reinforced concrete tall building." *Eng. Struct.*, 26(12), 1779–1794.

Li, Q. S., Xiao, Y. Q., and Wong, C. K. (2005). "Full-scale monitoring of typhoon effects on super tall buildings." *J. Fluids Struct.*, 20(5), 697–717.

Li, Q. S., Xiao, Y. Q., Wong, C. K., and Jeary, A. P. (2003a). "Field measurements of wind effects on the tallest building in Hong Kong." *Struct. Des. Tall Special Build.*, 12(1), 67–82.

Li, Q. S., Xiao, Y. Q., Wong, C. K., and Jeary, A. P. (2004b). "Field measurements of typhoon effects on a super tall building." *Eng. Struct.*, 26(2), 233–244.

Li, Q. S., Xiao, Y. Q., Wu, J. R., Fu, J. Y., and Li, Z. N. (2008). "Typhoon effects on super-tall buildings." *J. Sound Vib.*, 313(3–5), 581–602.

Li, Q. S., Yang, K., Wong, C. K., and Jeary, A. P. (2003b). "The effect of amplitude-dependent damping on wind-induced vibrations of a super tall building." *J. Wind Eng. Ind. Aerodyn.*, 91(9), 1175–1198.

Li, Q. S., Zhi, L. H., Tuan, A. Y., Kao, C. S., Su, S. C., and Wu, C. F. (2011). "Dynamic behavior of Taipei 101 tower: Field measurement and numerical analysis." *J. Struct. Eng.*, 10.1061/(ASCE)ST.1943-541X.0000264, 143–155.

Littler, J. D., and Ellis, B. R. (1992). "Full-scale measurements to determine the response of Hume point to wind loading." *J. Wind Eng. Ind. Aerodyn.*, 42(1–3), 1085–1096.

Ljung, L. (1987). *System identification: Theory for the user*, Prentice-Hall, Englewood Cliffs, NJ.

Marukawa, H., Kato, N., Fujii, K., and Tamura, Y. (1996). "Experimental evaluation of aerodynamic damping of tall buildings." *J. Wind Eng. Ind. Aerodyn.*, 59(2–3), 177–190.

Masciantonio, A., Isyumov, N., and Petersen, N. R. (1987). "Wind-induced response of a tall building and comparisons with wind tunnel predictions." *Structures Congress 87 related to Dynamics of Structures*, J. M. Roesset, ed., Univ. of Texas, Civ. Eng. Dept., Austin, TX.

Montpellier, P. R. (1996). "The maximum likelihood method of estimating dynamic properties of structures." M.S. thesis, Univ. of Western Ontario, London, ON, Canada.

Ni, Y. Q., and Zhou, H. F. (2010). "Guangzhou new TV tower: Integrated structural health monitoring and vibration control." *Structures Congress 2010*, Structural Engineering Institute (SEI), Reston, VA, 3155–3164.

Ohkuma, T., Marukawa, H., Niihori, Y., and Kato, N. (1991). "Full-scale measurement of wind pressures and response accelerations of a high-rise building." *J. Wind Eng. Ind. Aerodyn.*, 38(2–3), 185–196.

Pirnia, J. D., Kijewski, T., Abdelrazaq, A., Chung, J., and Kareem, A. (2007). "Full-scale validation of wind-induced response of tall buildings: Investigation of amplitude-dependent dynamic properties." *2007 Structures Congress: New Horizons and Better Practices*, (CD–ROM), Structural Engineering Institute (SEI), Reston, VA.

Rodgers, J. E., and Çelebi, M. (2006). "Seismic response and damage detection analyses of an instrumented steel moment-framed building." *J. Struct. Eng.*, 10.1061/(ASCE)0733-9445(2006)132:10(1543), 1543–1552.

Şafak, E. (1989a). "Adaptive modeling, identification, and control of dynamic structural systems. I: Theory." *J. Eng. Mech.*, 10.1061/(ASCE)0733-9399(1989)115:11(2386), 2386–2405.

Şafak, E. (1989b). "Adaptive modeling, identification, and control of dynamic structural systems. II: applications." *J. Eng. Mech.*, 10.1061/(ASCE)0733-9399(1989)115:11(2406), 2406–2426.

Şafak, E. (1991). "Identification of linear structures using discrete-time filters." *J. Struct. Eng.*, 10.1061/(ASCE)0733-9445(1991)117:10(3064), 3064–3085.

Şafak, E. (1993). "Response of a 42-story steel-frame building to the Ms=7.1 Loma Prieta earthquake." *Eng. Struct.*, 56(6), 403–421.

Şafak, E., and Çelebi, M. (1991). "Seismic response of Transamerica Building. II: System identification." *J. Struct. Eng.*, 10.1061/(ASCE)0733-9445(1991)117:8(2405), 2405–2425.

Şafak, E., and Çelebi, M. (1992a). "Recorded seismic response of Pacific Park Plaza. II: System identification." *J. Struct. Eng.*, 10.1061/(ASCE)0733-9445(1992)118:6(1566), 1566–1589.

Satake, N., Sude, K., Arakawa, T., Sasaki, A., and Tamura, Y. (2003). "Damping evaluation using full-scale data of buildings in Japan." *J. Struct. Eng.*, 10.1061/(ASCE)0733-9445(2003)129:4(470), 470–477.

Smith, R. J., and Willford, M. R. (2007). "The damped outrigger concept for tall buildings." *Struct. Des. Tall Special Build.*, 16(4), 501–517.

Tamura, Y. (2005). "Damping in buildings and estimation techniques." *6th Asia-Pacific Conf. on Wind Eng. (APCWE-VI)*, International Association for Wind Engineering (IAWE), Atsugi, Kanagawa, Japan, 193–213.

Tamura, Y. (2012). "Amplitude dependency of damping in buildings and critical tip drift ratio." *Int. J. High-Rise Build.*, 1(1), 1–13.

Tamura, Y., Suda, K., and Sasaki, A. (2000). "Damping in buildings for wind resistant design." *Int. Symp. on Wind and Structures for the 21st Century*, Techno-Press, Daejeon, Korea, 115–130.

Tamura, Y., and Suganuma, S. (1996). "Evaluation of amplitude-dependent damping and natural frequency of buildings during strong winds." *J. Wind Eng. Ind. Aerodyn.*, 59(2–3), 115–130.

Tamura, Y., and Yoshida, A. (2008). "Amplitude dependency of damping in buildings." (CD–ROM), *2008 Structures Congress: 18th Analysis and Comput. Specialty Conf.*, Structural Engineering Institute (SEI), Reston, VA.

Taoka, G. T., Scanlan, R. H., and Khan, F. R. (1975). "Ambient response analysis of some tall structures." *J. Struct. Div.*, 101(1), 49–65.

Wyatt, T. A. (1977). "Mechanisms of damping." *Symp. on Dynamic Behaviour of Bridges*, Transport and Road Research Laboratory, Crowthorne, U.K., 10–21.

Xu, Y. L., Chen, S. W., and Zhang, R. C. (2003). "Modal identification of Di Wang building under Typhoon York using the Hilbert-Huang transform method." *Struct. Des. Tall Special Build.*, 12(1), 21–47.

Xu, Y. L., and Zhan, S. (2001). "Field measurements of Di Wang Tower during Typhoon York." *J. Wind Eng. Ind. Aerodyn.*, 89(1), 73–93.

Yoon, S. W., and Ju, Y. K. (2004). "Dynamic properties of tall buildings in Korea." *Proc. of CTBUH 2004*, (CD–ROM), Council on Tall Buildings and Urban Habitat (CTBUH), Chicago.